23 November 2001

Chemical Physics Letters 349 (2001) 71–78

CHEMICAL PHYSICS LETTERS

www.elsevier.com/locate/cplett

Femtosecond ground state dynamics of gas phase N_2O_4 and NO_2

Igor Pastirk [1], Matthew Comstock, Marcos Dantus *

Department of Chemistry, Michigan State University, East Lansing, MI 48824, USA
Department of Physics and Astronomy, Michigan State University, East Lansing, MI 48824, USA

Received 25 June 2001; in final form 22 August 2001

Abstract

Non-resonant femtosecond time-resolved four-wave mixing (FWM) data on gas phase NO_2 and N_2O_4 are presented. The initial rotational dephasing is observed during the first picosecond after excitation. Fast vibrational dynamics (average value 133 ± 1 fs beats) are observed for dinitrogen tetroxide and are assigned to the ν_3 N–N stretching mode in the ground state (^1A_g). Rotational revivals on the picosecond time scale are recorded for both samples. No evidence of a long-lived excited state participation was found using photon echo (PE) or virtual echo (VE) pulse sequences with 800 nm laser pulses, however, NO_2 photoproducts were observed following N_2O_4 excitation.

1. Introduction

Nitrogen oxides (NO_x) have been the subjects of numerous studies primarily for their role in both stratospheric and tropospheric chemistry and in particular, their links to ozone photochemical cycles and smog formation. These relatively small molecules are especially interesting due to their complex spectroscopy as evidenced by theoretical and experimental studies of their ground and excited states [1–13]. All except NO have multidimensional potential energy surfaces and numerous curve crossings that result in vibronic chaos making these molecules very interesting to dynamicists.

The nitrogen dioxide/dinitrogen tetroxide monomer/dimer pair has received particular attention. The dimer is favored at higher pressures and lower temperatures. At 1 atm and room temperature the equilibrium concentration of NO_2 is about 16% [6,14]. Dinitrogen tetroxide is particularly intriguing because of its unusually long N–N bond (1.776 Å, gas phase) [15,16] and the fact that the ONO bond length and angle are identical to those of the monomer (see Fig. 1). Because of its (D_{2h}) symmetry, N_2O_4 does not have a permanent electric dipole moment. The dissociation energy of the N–N bond is 0.59 eV and its first electronic resonance is at 340 nm [1]. It has been proposed [6] that the use of off-resonance

* Corresponding author. Fax: +1-517-353-1793.
E-mail address: dantus@msu.edu (M. Dantus).
[1] Affiliated to the Institute for Nuclear Sciences 'VINCA', Belgrade, F.R. Yugoslavia.

0009-2614/01/$ - see front matter
PII: S0009-2614(01)01107-1

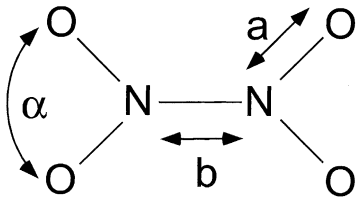

Fig. 1. Sketch of the N_2O_4 molecule: (a) the N–O distance is 1.19 Å; (b) the N–N bond is 1.776 Å, and the angle α is 134.6°, from [15].

excitation should make it possible to directly probe the dimer at room temperature. Most of the vibrational frequencies for these molecules are established and assigned [3–6], but there is still some disagreement between experiment and theory on several modes. Time-resolved rotational dynamics of NO_2 were measured by Sarkisov et al. [17] using femtosecond Raman-induced polarization spectroscopy. The photodissociation dynamics of NO_2 were recently studied using ultrafast methods [18,19]. Here we exploit the ability to detect low frequency Raman modes of short-lived species and to measure high accuracy rotational constants by femtosecond time-resolved four wave mixing (FWM) to study the ground state dynamics of N_2O_4/NO_2.

2. Experimental

The experiments were performed using a regeneratively amplified femtosecond titanium–sapphire laser system (Fig. 2). The output from a continuous wave Nd:YVO_4 laser (Millennia – Spectra Physics Laser) pumps the femtosecond titanium–sapphire oscillator (KM Labs), capable of producing <15 fs pulses at 90 MHz. This output was amplified by a regenerative amplifier (Spitfire – Spectra Physics Lasers) pumped by 1 kHz Nd:YLF laser (Evolution-X – Spectra Physics Lasers). Amplified pulses centered at 805 nm were close to transform limited and had a maximum energy of 0.8 mJ/pulse and time duration of 50 fs. Characterization of the pulses was performed both with non-collinear autocorrelation and frequency resolved optical grating [20]. Both methods confirmed that the pulses were shorter than 50 fs

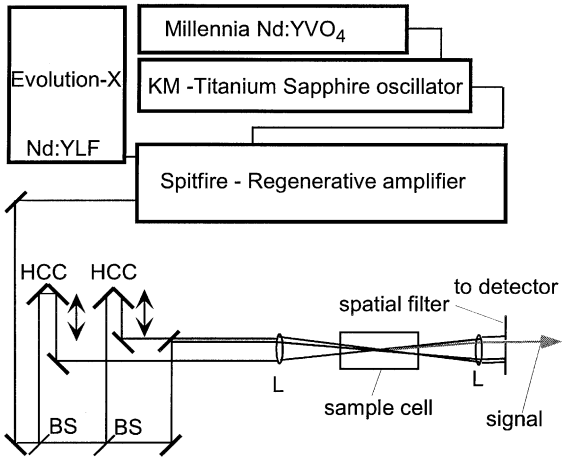

Fig. 2. Setup used for the femtosecond FWM experiments. HCC are hollow corner cube retro-reflectors and BS are beam splitters.

measured at full-width half-maximum and had no residual chirp. The output was split into three beams using dielectric beam splitters and recombined in a forward-box geometry (see Fig. 2). In all experiments the output beam was attenuated to ~60 μJ per pulse measured before splitting. Two beams were overlapped in time and space to form a transient grating in the sample while the third one was time delayed with a computer controlled actuator. This configuration allows transient grating (TG) and reverse transient grating (RTG) experiments. When the initial two pulses are not overlapped in time, other types of FWM experiments (photon echo (PE) and virtual echo (VE)) are possible [21].

The event when all three pulses overlap in time is referred to as time zero. The three 10 mm diameter beams were focused into a 6 in. long custom-designed quartz cell containing the gaseous sample by a 2 in. diameter lens with focal length of 50 cm. The temperature was controlled with heating tape surroundings the entire cell. The FWM signal beam was spatially filtered by a set of irises, collimated and sent into a spectrometer (Triax 320, JobinYvon). Before reaching the entrance slit of the spectrometer, the signal was attenuated by a neutral density filter of OD = 1–2. The signal was then dispersed by the spectrometer's grating, and was registered by a 2000 × 800

pixel liquid nitrogen cooled CCD. The entrance slit of the spectrometer was 100 μm (0.8 nm resolution). The wavelength range on the CCD in this setup (grating dictated) was about 60 nm. In order to preserve disk space, every 20 pixels were binned together. For the shorter scans (~1–2 ps duration) the frequency-dispersed signal was recorded every 10 fs, while for the longer scans the time-steps were 20 fs. Signal was registered for each time delay with an integration time of 100 ms. Each data set is the average of several such scans.

The sample (99.1% N_2O_4) was obtained from Sigma–Aldrich and used without further purification. The sample cell was pumped out to 10^{-5} Torr on the vacuum line and filled directly from the lecture bottle. There was no experimental evidence of contamination. Experiments were performed at different sample pressures. All the data presented here were obtained with a cell that was loaded to an initial pressure of 400 Torr at room temperature.

3. Results

In the gaseous state, the N_2O_4 and NO_2 molecules are in thermodynamic equilibrium (at room temperature $K = 8.8$ atm^{-1}) [22]. We controlled the temperature and pressure of the sample cell from 294 K (80% N_2O_4) to 363 K (94% NO_2), values from [14]. A change in optical density of the sample at 805 nm from 0.045 (294 K) to 0.071 (363 K) was observed and was not considered substantial to qualitatively affect the measurements. Some experiments were carried out with a cell filled to 760 Torr. The overall signal level was somewhat smaller due to the increased OD leading to absorption of the excitation photons. The transients yielded qualitatively identical results, but required a higher temperature to obtain good NO_2 signal (383 K), probably due to a change in the equilibrium conditions and some re-absorption of the signal. It is necessary to note that it is impossible to have 100% pure gaseous N_2O_4 in the cell because of the aforementioned equilibrium.

In Fig. 3 we present frequency-dispersed transients obtained as a function of time delay between the two time-overlapped pulses and the third pulse for NO_2 (3a) and N_2O_4 (3c). In the two-dimensional contour plots (a and c) the spectrum of the signal in the region from 780 to 830 nm is registered versus delay time every 10 fs. The dark current level of the CCD was subtracted from these data. The intensity scale is logarithmic to highlight the weaker features. In the case of NO_2 (Fig. 3a) there is a broad, featureless peak 160 fs after time zero [17] as well as another at 500 fs. Fig. 3b shows the frequency-integrated (780–830 nm) transient signal. These features (Fig. 3a,b) can be assigned to the initial rotational dephasing in the sample and are consistent with results for off-resonance FWM signal [23,24]. Measurements for N_2O_4 were collected in the same manner as described for NO_2 and are presented in Fig. 3c,d. These results show, in addition to a broad rotational dephasing envelope, a series of beats with an average period of 133 fs. The beats are detectable up to 3 ps after time zero but with much lower intensity.

Long time scans were performed at 363 K (NO_2) or 294 K (N_2O_4). We present data in the time delay range from 9 to 42 ps in Fig. 4. The transients show the frequency-integrated intensity recorded in the 785–825 nm range as a function of time delay. Note that the vertical axis (intensity) is logarithmic. The NO_2 data presented in Fig. 4a show rotational recurrences every 19.680 ps with half recurrences in between (9.840 ps). The transient in Fig. 4b, taken at 294 K, exhibits similar features with the same periodicity. The recurrences observed at 294 K are about six times lower in intensity than those observed for NO_2 at 363 K taking into account the attenuation filter used for the higher temperature transients. The transients for both temperatures were taken under identical laser conditions except for attenuation. This results in slightly different background and noise levels between the two transients. In this range of time delays both data sets exhibit rotational recurrences that can be assigned to NO_2. Under close examination some differences are observed in the shape of the rotational recurrences obtained in the two transients. The differences are especially clear at the half recurrence observed in both transients near 29.5 ps (see Fig. 4).

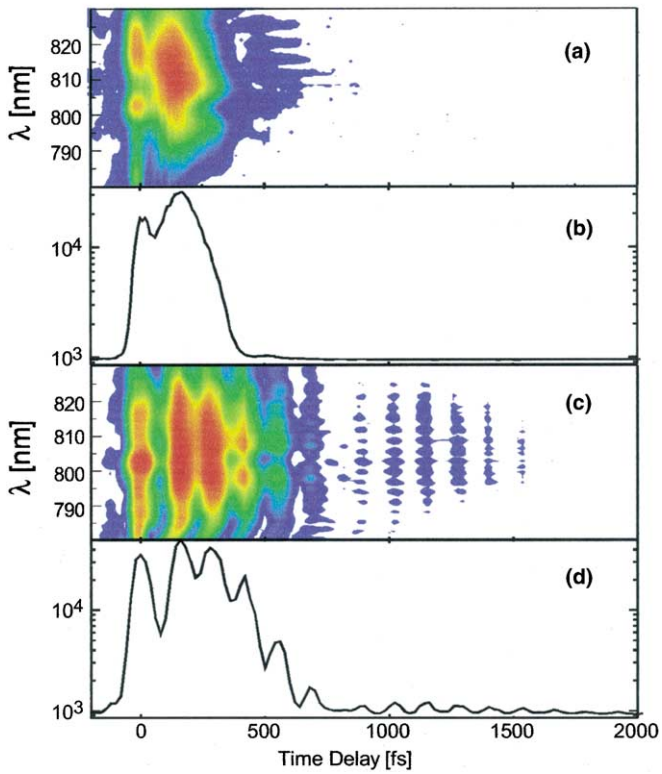

Fig. 3. Experimental time-resolved FWM signal obtained during the first 2 ps: (a) frequency dispersed signal obtained as a function of time delay for NO_2; (b) frequency integrated NO_2 data as a function of time delay; (c) frequency dispersed signal as a function of time delay for N_2O_4; (d) frequency integrated N_2O_4 data as a function of time delay. For all scans, the signal intensity is plotted on a logarithmic scale.

Nitrogen dioxide is an asymmetric top molecule, but the similarity of the B and C constants allows us to view it as a symmetric top with $B_{ave} = (B + C)/2$. From the observed rotational recurrences of 19.680 ps (9.840 ps half recurrences) in the long time delay transient of NO_2 (Fig. 4a) we can calculate the average rotational constant as $B_{ave} = 1/4c\tau_{rec}$, where c is the speed of light and τ_{rec} is the time between rotational recurrences [23,24]. The obtained value is 0.42343 ± 0.00007 cm^{-1}. This value compares favorably to the reported experimental (0.42202 cm^{-1}) [25] and theoretical (0.423325 cm^{-1}) [7] values calculated for B_{ave}, respectively. Simulations based on the semiclassical formalism outlined in [23,24] and the average rotational constant for NO_2 using the literature values are in general agreement with the observed data (see vertical lines in Fig. 4). The rotational recurrences obtained at longer time delays ($\tau > 40$ ps) exhibit a more complex modulation that cannot be simulated with a symmetric top approximation, even though their positions can be exactly reproduced.

In the case of N_2O_4, the signal obtained at long time delays is more complex. The small features at 9.840 and 19.680 ps (Fig. 4b) could be assigned to rotational recurrences originating from the 16% NO_2 molecules present at room temperature. The positions of these features coincide precisely with the rotational recurrences of NO_2, however, the signal intensity is about one order of magnitude stronger than expected based on the observed intensity at 363 K and because of the square dependence on number density for these measurements [23,24]. Furthermore, there are some subtle differences in the shape of the recurrences;

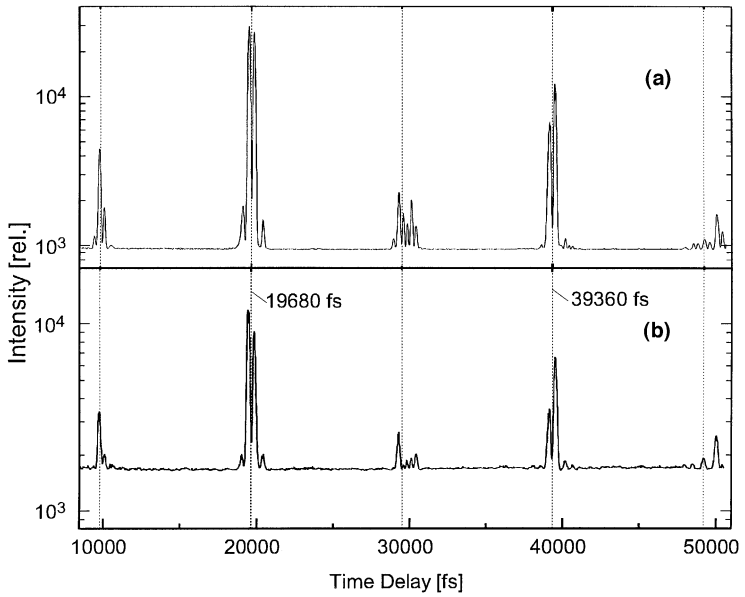

Fig. 4. Experimental time-resolved and frequency-integrated FWM signal (a) NO_2 and (b) N_2O_4 taken at 363 and 294 K, respectively. Note the subtle differences in the shape of the rotational recurrences obtained for both cases. The signal intensity is plotted on a logarithmic scale. The vertical lines indicate the position of the rotational recurrences obtained from a simulation using $B_{ave} = (B + C)/2$.

for example the half recurrence at 29.5 ps in Fig. 4, leading us to consider assigning a significant contribution of these features to photoproducts that result from excitation by the first two pulses. The N–N bond dissociation energy is only 0.59 eV while the photon energy of each pulse is 1.54 eV. The principal axis of the NO_2 moieties is aligned with the N–N bond of N_2O_4, therefore, the initial rotational alignment would be preserved in the photodissociation process. The product NO_2 molecules formed by photodissociation would realign and become 'visible' to the third pulse at the same time delays as the thermal NO_2 molecules originally in the sample, but would have a different rotational temperature. There is a possibility that multiphoton excitation yields NO_2 molecules in the $^2B_2$ excited state, which has slightly different (and still not exactly determined) rotational constants.

The initial rotational dephasing observed during the first picosecond is vibrationally modulated. The time between first five beats is 158, 125, 131 and 135 fs. Fourier transform of the signal results in a single broad feature centered at 234 cm^{-1}. The experimentally obtained value for the N–N stretching mode from gas-phase Raman spectroscopy is 254 cm^{-1} [6], and from high resolution FTIR [26] and Raman [27] spectra on solid N_2O_4 is 281.3 cm^{-1}. The only other frequency that could be implicated is the NO_2 rocking mode $\nu_{10} =$ 265.5 cm^{-1} [26]; however, this mode is not Raman active and therefore not observed in our measurements. Applying the maximum entropy method (MEM) of analysis [28] on the same set of data yielded two frequencies; 238.5 and 251.8 cm^{-1}. These two values were consistently obtained following analysis of different data sets (not shown). The observed wave packet motion involves at least three vibrational levels in the ground state. The difference between the two frequencies obtained by MEM gives the anharmonicity of this vibrational mode. Presumably, the 251.8 cm^{-1} value corresponds to the lowest level(s), consistent with the reported gas phase value, and the 238.5 cm^{-1} value to the higher levels. Our findings are consistent with the extremely

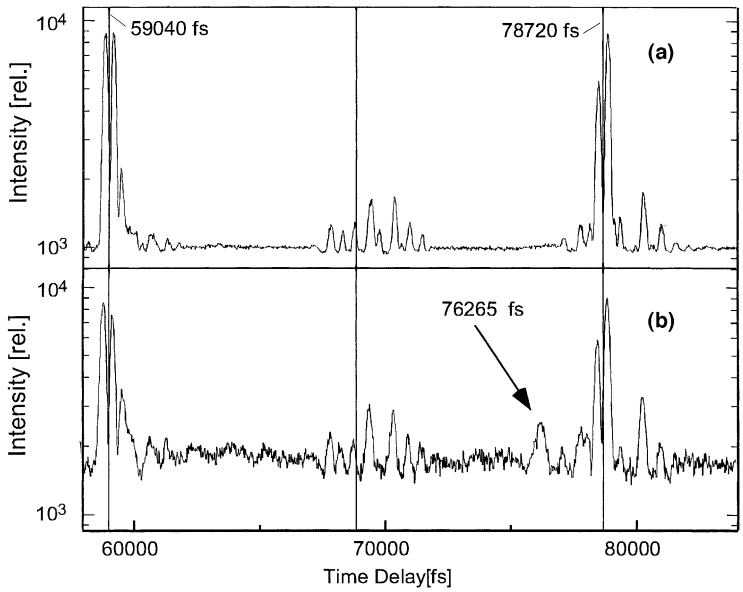

Fig. 5. Experimental time-resolved and frequency-integrated signal obtained at 363 K (a) and 294 K (b). The main difference between the two transients, after the first two picoseconds occurs, at 76.265 ps and is indicated by an arrow. Both intensity axes are plotted on a logarithmic scale. Some fine differences are observed in the modulation of the rotational recurrences but not in their position.

large anharmonicity of N_2O_4 [29]. We leave a more detailed analysis for future work where we hope to get even higher quality data.

Only one rotational recurrence feature was observed after the first picosecond that can be assigned to N_2O_4. At 76.265 ps (Fig. 5) a small feature is present in the room temperature sample that is clearly absent at higher temperatures. This feature gains in intensity compared to the one at 78.540 ps (NO_2 recurrence) if the temperature of the sample is lowered to 0 °C (data not shown). The lower temperature drop shifts the equilibrium further towards the dimer. If a semiclassical model and available rotational constants [4,9] are used, it is possible to simulate this recurrence. The experimental data showed no evidence of a half recurrence at 38 ps. Scans taken for time delays of up to 160 ps showed no other feature that could be distinctly assigned to N_2O_4. One possible reason for the absence of N_2O_4 rotational recurrences at long time delays (>100 ps) is the rapid thermodynamic exchange $2NO_2 \rightleftharpoons N_2O_4$; which we estimate to be $\tau < 0.1$ ns at 300 K.

4. Discussion

The signal observed for both molecules is primarily non-resonant and therefore depicts ground state dynamics. Experiments were carried out at both temperatures: PE and VE pulse sequences [30,31], were performed but yielded no significant feature other than the time zero signal. If the experiments shown here had involved a resonant one-photon transition to the $^2B_2$ state of NO_2, the PE and VE signals would have revealed it.

The absorption cross-section of NO_2 at 800 nm is very small [32,33]. The reported and calculated values of the B and C rotational constants for the $^2B_2$ state are very dissonant [32], and fall in the range from 0.458 to 0.548 cm^{-1} and 0.38 to 0.449 cm^{-1}, respectively. If these transitions were involved additional rotational recurrences corresponding to these values would have been observed in the time-resolved FWM transients. Close examination of the data did not reveal any other features except for the aforementioned recurrences every 19.680 ps. Given that homodyne detected

FWM signal depends on the transition dipole moment to the eighth power [23,24] this process is not likely to be detected by our setup.

In conclusion, the average rotational constant measured from our experiments of 0.42343 cm^{-1} reflects the average $(B + C)/2$ rotational constant of NO_2 in the ground state. The experiments at room temperature (N_2O_4) allowed us to measure the frequency of the N–N stretch of 234 cm^{-1} and perhaps the anharmonicity of this unusual bond. The next electronic state known is the $^3B_{3u}$ which is reached with photon energies >3 eV [13] and would require two photon transitions. There is no evidence in our data of single or multiphoton transitions to a long-lived excited state. However, excitation to a dissociative state would be difficult to rule out. Perhaps the negative time delay shoulder in the N_2O_4 transient in Fig. 3d and not found in the NO_2 transient in Fig. 3b is the evidence of this dissociative pathway.

A new set of experiments is planned with shorter (~20 fs) and tunable pulses from an optical parametric oscillator source (NOPA – ClarkMXR). The goals are to explore the dynamics of the $^2B_2$ excited state of NO_2 and its curve-crossing dynamics with the ground state. We will revisit the evidence for photodissociation and the dissociation dynamics in N_2O_4. We will adapt the available methods and programs [34,35] used in the analysis of rotational coherence spectroscopy to fit our data and determine differences between room temperature and photoproduced NO_2. We will re-examine the rotational recurrence for N_2O_4 in order to refine the degree of planarity. At present the effective angle of torsion has been determined to be $5° \pm 7°$ by electron diffraction [15].

Acknowledgements

We want to thank Dr. Vadim V. Lozovoy for a critical review and comments on the work presented here and Katherine A. Walowicz for implementing and fine tuning the frequency dispersed data acquisition system and for proof reading the manuscript. This research was funded by grants from the National Science Foundation (CHE-9812584) and by the Chemical Sciences, Geosciences and Biosciences Division, Office of Basic Energy Sciences, Office of Science, U.S. Department of Energy. MD is a Lucille and David Packard Science and Engineering Fellow, a Camille Dreyfus Teacher–Scholar, and an Alfred P. Sloan Fellow.

References

[1] T.C. Hall, F.R. Blacet, J. Chem. Phys. 20 (1952) 1745.
[2] N.R. Weiner, E.R. Nixon, J. Chem. Phys. 26 (1957) 906.
[3] C.H. Bibart, G.E. Ewing, J. Chem. Phys 61 (1974) 1284.
[4] D. Luckhaus, M. Quack, Chem. Phys. Lett. 199 (1992) 293.
[5] F. Melen, F. Pokorni, M. Herman, Chem. Phys. Lett. 194 (1992) 181.
[6] C. Dyer, P.J. Hendra, Chem. Phys. Lett. 233 (1995) 461.
[7] T. Kato, J. Chem. Phys. 105 (1996) 4511.
[8] A. Stirling, I. Papai, J. Mink, D.R. Salahub, J. Chem. Phys. 100 (1994) 2910.
[9] J.L. Domenech, A.M. Andrews, S.P. Belov, G.T. Fraser, W.J. Lafferty, J. Chem. Phys. 100 (1994) 6993.
[10] S.S. Wesolowski, J.T. Fermann, T.D. Crawford, H.F. Schaefer, J. Chem. Phys. 106 (1997) 7178.
[11] B. Kirmse, A. Delon, R. Jost, J. Chem. Phys. 108 (1998) 6638.
[12] B.F. Parsons, S.L. Curry, J.A. Mueller, P.C. Ray, L.J. Butler, J. Chem. Phys. 111 (1999) 8486.
[13] J.A. Mueller, M.L. Morton, S.L. Curry, J.P.D. Abbatt, J.B. Butler, J. Phys. Chem. 104 (2000) 4825.
[14] C. Streuli, P. Averell, The Analytical Chemistry of Nitrogen and its Compounds. Part I, Wiley, New York, 1970.
[15] K.B. Borisenko, M. Kolonits, B. Rozsondai, I. Hargittai, J. Mol. Struct. 413 (1997) 121.
[16] A. Kvick, R.K. McMullan, M.D. Newton, J. Chem. Phys. 76 (1982) 3754.
[17] O.M. Sarkisov, D.G. Tovbin, V.V. Lozovoy, F.E. Gostev, A.A. Titov, S.A. Antipin, S.Y. Umanskiy, Chem. Phys. Lett. 303 (1999) 458.
[18] J.A. Davies, J.E. LeClaire, R.E. Continetti, C.C. Hayden, J. Chem. Phys. 111 (1999) 1.
[19] J.A. Davies, R.E. Continetti, D.W. Chandler, C.C. Hayden, Phys. Rev. Lett. 84 (2000) 5983.
[20] R. Trebino, D.J. Kane, J. Opt. Soc. Am. A 10 (1993) 1101.
[21] I. Grimberg, V.V. Lozovoy, M. Dantus, S. Mukamel, J. Phys. Chem. (2001) (in press).
[22] W.L. Jolly, The Inorganic Chemistry of Nitrogen, Benjamin, New York, 1964.
[23] E.J. Brown, Q. Zhang, M. Dantus, J. Chem. Phys. 110 (1999) 5772.
[24] M. Dantus, Ann. Rev. Phys. Chem. 52 (2001) 639.

[25] G. Herzberg, Molecular Spectra and Molecular Structures. III. Electronic Spectra and Electronic Structure of Polyatomic Molecules, Krieger, Malbar, FL, 1991.
[26] B. Andrews, A. Anderson, J. Chem. Phys. 74 (1981) 1534.
[27] F. Bolduan, H.J. Jodi, A. Loewenschuss, J. Chem. Phys. 80 (1984) 1739.
[28] W.H. Press, S.A. Teukolsky, W.T. Vetterling, B.P. Flannery, Numerical Recipes in C, Cambridge University Press, New York, 1992.
[29] M. Hepp, R. Georges, M. Herman, J.M. Flaud, W.J. Lafferty, J. Mol. Struct. 517 (2000) 171.
[30] V.V. Lozovoy, I. Pastirk, E.J. Brown, B.I. Grimberg, M. Dantus, Int. Rev. Phys. Chem. 19 (2000) 531.
[31] I. Pastirk, V.V. Lozovoy, M. Dantus, Chem. Phys. Lett. 333 (2001) 76.
[32] G.D. Gillispie, A.U. Khan, J. Chem. Phys. 65 (1976) 1624.
[33] J. Lievin, A. Delon, R. Jost, J. Chem. Phys. 108 (1998) 8931.
[34] P.W. Joireman, L.L. Connel, S.M. Ohline, P.M. Felker, J. Chem. Phys. 96 (1992) 4118.
[35] M.F. Gelin, V.A. Tolkachev, A.P. Blokhin, Chem. Phys. 255 (2000) 111.